PROCEEDINGS OF SCIENCE

Rare $b \to s\ell^+\ell^-$ analyses with electrons

Albert Puig Navarro[*†]
Physik-Institut, Universität Zürich, Zürich (Switzerland)
E-mail: albert.puig@cern.ch

Rare $b \to s\ell^+\ell^-$ decays are flavour-changing neutral-current processes that are forbidden at the lowest perturbative order in the Standard Model (SM). As a consequence, new particles in SM extensions can significantly affect the branching fractions of these decays and their angular distributions, as well as affect the coupling of the electroweak gauge bosons of the SM to leptons in a non-universal way. Tensions have been observed at the LHCb experiment, in particular when comparing $b \to s\mu^+\mu^-$ and $b \to se^+e^-$ decays. Recent results from the LHCb experiment in this area are presented, with special focus on the experimental techniques used to study decays with electrons in the final state.

LHCb-PROC-2018-015
06/07/2018

The International Conference on B-Physics at Frontier Machines - BEAUTY2018
6-11 May, 2018
La Biodola, Elba Island, Italy

[*]Speaker.
[†]On behalf of the LHCb collaboration.

1. Introduction

Quarks and leptons in the Standard Model (SM) are organized in *flavours*. Changes between flavours can only occur through the charged-current weak interaction, causing transitions between same-charge fermions to only be allowed through second order (loop) processes [1]. As a consequence, processes involving *flavour-changing neutral currents* (FCNC) are predicted to be rare within the SM.

Since many observables related to this type of decays can be predicted in the SM with small theoretical uncertainty, loop-mediated processes allow for a precise indirect access to new particles at large scales and provide excellent complementarity to direct searches of new phenomena. Many models of New Physics (NP) predict significant changes in the measured quantities, making the study of rare decays of flavoured hadrons an ideal laboratory for studying physics beyond the SM. In particular, semileptonic $b \to s(d)\ell^+\ell^-$ decays have been extensively studied at the LHC, where the signal yields of many modes are large enough for precision measurements. Results on differential branching fractions and angular distributions, as well as ratios between muonic and electronic decays, have provided many constraints on NP models and have yielded interesting tensions with the SM. These latter ratios are expected to be very close to unity[1] due to the fact that in the SM the gauge bosons couple equally to different lepton flavours.

In this context, the study of $b \to s\ell^+\ell^-$ transitions including electrons is of the utmost importance, not only to test lepton flavour universality, but also because they allow to access the photon polarisation through the study of $B^0 \to K^{*0}e^+e^-$ decays at very low dilepton mass squared (q^2). Additionally, it is interesting to study lepton flavour violation decays, such as $B \to e\mu$, forbidden in the SM but with significant branching fractions in many of its extensions.

2. Reconstructing and selecting electrons in the LHCb experiment

The LHCb detector [2, 3] is a single-arm forward spectrometer covering the pseudorapidity range $2 < \eta < 5$, designed for the study of particles containing b or c quarks. The detector includes a high-precision tracking system consisting of a silicon-strip vertex detector surrounding the pp interaction region, a large-area silicon-strip detector located upstream of a dipole magnet with a bending power of about 4 Tm, and three stations of silicon-strip detectors and straw drift tubes placed downstream of the magnet. The tracking system provides a measurement of momentum, p, of charged particles with a relative uncertainty that varies from 0.5% at low momentum to 1.0% at 200 GeV/c. The minimum distance of a track to a primary vertex (PV), the impact parameter (IP), is measured with a resolution of $(15 + 29/p_{\mathrm{T}})$ mm, where p_{T} is the component of the momentum transverse to the beam, in GeV/c. Different types of charged hadrons are distinguished using information from two ring-imaging Cherenkov detectors. Photons, electrons and hadrons are identified by a calorimeter system consisting of scintillating-pad and preshower detectors, an electromagnetic calorimeter and a hadronic calorimeter. Muons are identified by a system composed of alternating layers of iron and multiwire proportional chambers.

Electrons are reconstructed using the tracking system and identified by the calorimeter system. Their main feature is that they emit a much larger amount of bremsstrahlung with respect to

[1] Except from very small Higgs penguin contributions and difference in phase space due to the lepton masses.

their muon counterparts, that results in a significant degradation of the momentum resolution and consequently in a degradation of the B mass resolution. If the radiation occurs downstream of the magnet, the electron momentum, measured from the bending of its trajectory in the magnet, is correctly measured; if it happens upstream of the magnet, the electron momentum, evaluated after the photon emission, is corrected using a dedicated bremsstrahlung recovery procedure that extrapolates the track to the electromagnetic calorimeter and searches for energy clusters in its vicinity. In the case of dielectron final states, candidates can be classified according to how many of the electrons have an associated recovered bremsstrahlung photons (zero, one or two) and each of these cases needs to be treated separately, as the different energy resolutions lead to different B mass shapes.

The online event selection consists of a hardware trigger stage, based on information from the calorimeter and muon systems, followed by a software stage, which applies a full event reconstruction. In the first stage, events are required to have a muon with high p_{T} (larger thab $1.8\,\mathrm{GeV}/c$) or a hadron, photon or electron with high transverse energy in the calorimeters. These latter requirements on the transverse energy are quite high, between 2.5 and 3 GeV, and they result in a large loss of efficiency when selecting $b \to se^+e^-$ decays. To partially recover from this effect, events where the hadronic part of the decay is responsible for firing the hadronic hardware trigger (also with a high transverse energy threshold, typically above 3.5 GeV) and events where other particles produced in the pp collision are responsible for firing any hardware trigger are also used. While this improves the selection efficiency, it also requires to analyze each of the subsamples separately, adding significant complexity to the analyses.

3. Angular analysis of $B^0 \to K^{*0}e^+e^-$

The LHCb collaboration has measured the angular distributions of the $B^0 \to K^{*0}e^+e^-$ decay in the low-q^2 region with data collected during the first run of the LHC [4]; to cope with the limited signal yield, the full $B^0 \to K^{*0}e^+e^-$ angular distributions were simplified by transforming the ϕ angle to $\tilde{\phi} = \phi + \pi$ if $\phi < 0$, obtaining

$$\begin{aligned}\frac{1}{\mathrm{d}(\Gamma+\bar{\Gamma})\,\mathrm{d}q^2}\frac{\mathrm{d}^4(\Gamma+\bar{\Gamma})}{\mathrm{d}q^2\,\mathrm{d}\cos\vartheta_\ell\,\mathrm{d}\cos_K\,\mathrm{d}\tilde{\phi}} = \frac{9}{16\pi}\Big[&\frac{3}{4}(1-F_{\mathrm{L}})\sin^2\vartheta_\ell + F_{\mathrm{L}}\cos^2\vartheta_K + \\ &\Big(\frac{1}{4}(1-F_{\mathrm{L}})\sin^2\vartheta_K - F_{\mathrm{L}}\cos^2\vartheta_K\Big)\cos\vartheta_\ell + \\ &\frac{1}{2}(1-F_{\mathrm{L}})A_T^{(2)}\sin^2\vartheta_K\sin^2\vartheta_\ell\cos^2\tilde{\phi} + \\ &(1-F_{\mathrm{L}})A_T^{\mathrm{Re}}\sin^2\vartheta_K\cos\vartheta_\ell + \\ &\frac{1}{2}(1-F_{\mathrm{L}})A_T^{\mathrm{Im}}\sin^2\vartheta_K\sin^2\vartheta_\ell\sin^2\tilde{\phi}\Big].\end{aligned} \tag{3.1}$$

The results, obtained through simultaneous fits to the three abovementioned hardware trigger

categories and shown in Fig. 1 are found to be

$$\begin{aligned} F_{\rm L} &= 0.16 \pm 0.06 \pm 0.03, \\ A_T^{(2)} &= -0.23 \pm 0.23 \pm 0.05, \\ A_T^{\rm Re} &= 0.10 \pm 0.18 \pm 0.05, \\ A_T^{\rm Im} &= 0.14 \pm 0.22 \pm 0.05. \end{aligned} \tag{3.2}$$

These measurements are compatible with the SM predictions [5, 6] and are an important ingredient to measure the photon polarisation thanks to the low lepton mass, providing some of the best constraints up-to-date [7].

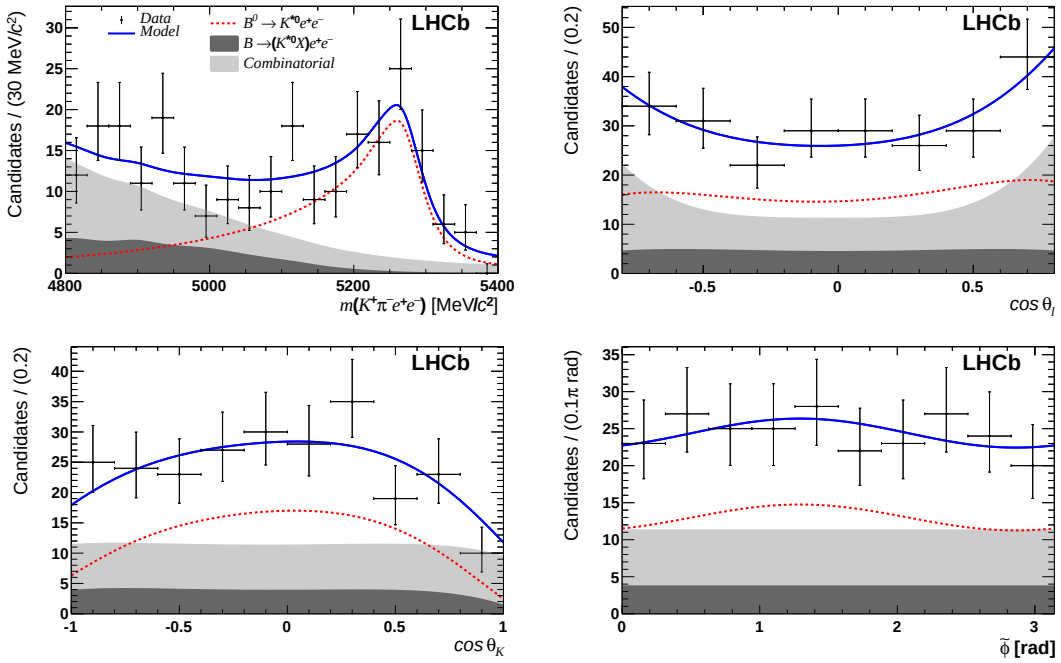

Figure 1: Distributions of the $K^+\pi^-e^+e^-$ invariant mass and angular variables for the $B^0 \to K^{*0}e^+e^-$ decay, with the three trigger categories grouped together. The angles shown are described in Ref. [4].

4. Lepton flavour universality measurements in LHCb

Ratios of $b \to s\ell^+\ell^-$ branching fractions, defined as

$$R_X = \frac{\mathscr{B}(b \to X\mu^+\mu^-)}{\mathscr{B}(b \to Xe^+e^-)}, \tag{4.1}$$

are predicted to be 1 with $\mathscr{O}(1\%)$ precision in the $1.1 < q^2 < 6.0\,{\rm GeV}^2/c^4$ range [8]. As a consequence, they constitute very powerful null tests of the SM.

In 2014, the LHCb collaboration measured R_K in the q^2 range $1 < q^2 < 6\,{\rm GeV}^2/c^4$ to be $0.745^{+0.090}_{-0.074}\,({\rm stat}) \pm 0.036\,({\rm syst})$ [9], 2.6σ away from the SM prediction. This discrepancy, combined with the 4.0σ enhancement of τ with respect to μ in tree-level $B^+ \to D^{(*)}\ell^+\nu_\ell$ decays observed by

BaBar, Belle and LHCb [10], prompted great interest in these types of measurements. A mesurement of $R_{K^{*0}}$ followed in 2017 [11]; in this latter case, the study was performed in two different bins of q^2: a *low-*q^2 region going from 0.045 to 1.1 GeV^2/c^4, and a *central* bin from 1.1 to 6.0 GeV^2/c^4.

The R_X ratios (for example $R_{K^{*0}}$) are measured as double ratios with respect to the corresponding resonant modes,

$$R_{K^{*0}} = \frac{\mathscr{B}(B^0 \to K^{*0}\mu^+\mu^-)}{\mathscr{B}(B^0 \to K^{*0}J/\psi(\to \mu^+\mu^-))} \Big/ \frac{\mathscr{B}(B^0 \to K^{*0}e^+e^-)}{\mathscr{B}(B^0 \to K^{*0}J/\psi(\to e^+e^-))}, \tag{4.2}$$

in order to cancel most of the experimental systematic uncertainties arising from the differences in reconstructing electrons and muons. Additionally, the electron modes are studied in categories of bremsstrahlung photons and hardware trigger, as already mentioned.

Two ingredients are needed for these measurements: signal yields and their corresponding efficiencies. In order to measure efficiencies, simulated events are used. Imperfections in the simulation, arising from kinematic effects, such as the mismodelling of the B transverse momentum, the response of the hardware trigger, reconstruction effects, and particle identification are calibrated using data driven techniques and control modes. Even if a large fraction of these effects are cancelled thanks to the double ratio strategy, differences between electrons and muons, especially in reconstruction and trigger response, need to be carefully corrected to avoid any biases by using resonant control modes.

The control of the absolute scale of the efficiencies after these calibrations is checked as a function of various kinematical variables using the resonant modes by measuring the ratio

$$r_{J/\psi} = \frac{\mathscr{B}(B^0 \to K^{*0}J/\psi(\to \mu^+\mu^-))}{\mathscr{B}(B^0 \to K^{*0}J/\psi(\to e^+e^-))}, \tag{4.3}$$

which is unity in the SM. This is an extremely stringent test, as no cancellations occur like in the case of the double ratio, and it is considered as the golden standard in these measurements. Further cross checks are the measurement of $R_{\psi(2S)}$, also expected to be unity and which allows to test the double ratio method in a different range of q^2, and the branching fractions of $B^0 \to K^{*0}\mu^+\mu^-$ and $B^0 \to K^{*0}\gamma(\to e^+e^-)$, which are compared to their measured values to check that the muon mode and the contamination from radiative decays are well under control.

Signal and control mode yields are obtained from unbinned maximum likelihood fits to the $K^+\pi^-\ell^+\ell^-$ invariant masses. While the muon channels, shown in Figs. 2 and 3, present very clean distributions with small background contributions due to the very narrow mass peak, the electron modes have long low-mass tails due to the large resolution of the electron momentum, as can be seen by comparing the invariant mass distributions of the J/ψ modes in Fig. 2. This results in a larger contamination from *partially reconstructed* backgrounds, *i.e.*, backgrounds coming from B decays where one or more particles have not been reconstructed, shifting them to lower mass values, as can be already seen in Fig. 1.

To address the issue of the background contamination due to the long tails, a special technique has been developed in the $R_{K^{*0}}$ analysis. The event topology sketched in Fig. 4 shows that the ratio of the momentum components transverse to the direction of flight of the B^0 candidate is expected to be unity if all bremsstrahlung photons have been properly recovered. Since bremsstrahlung photons don't modify the direction of the dielectron system, one can use this ratio to correct the dielectron

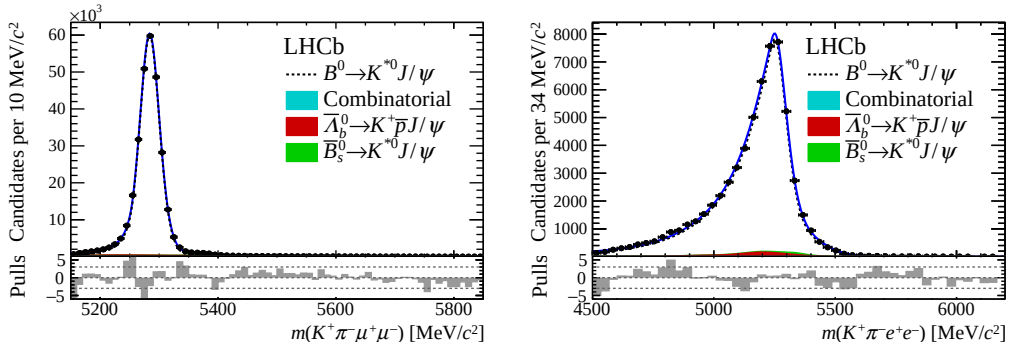

Figure 2: Fit to the invariant mass distributions of (left) $K^+\pi^- J/\psi(\to \mu^+\mu^-)$ and (right) $K^+\pi^- J/\psi(\to e^+e^-)$. Taken from Ref. [11].

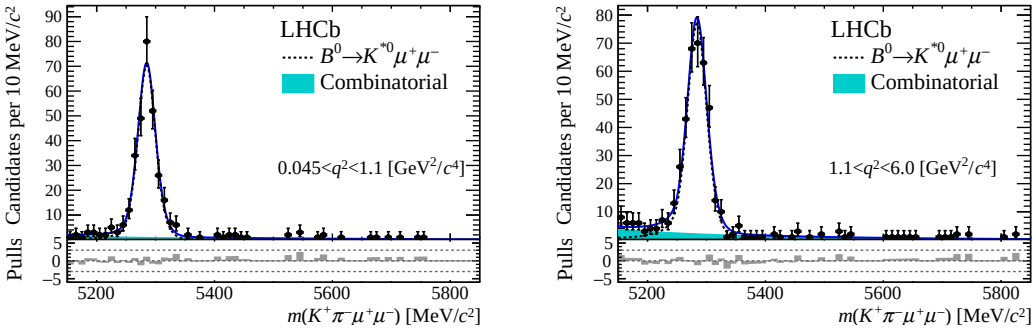

Figure 3: Fit to the invariant $K^+\pi^-\mu^+\mu^-$ mass distributions of $B^0 \to K^{*0}\mu^+\mu^-$ in the (left) low- and (right) central-q^2 bins. Taken from Ref. [11].

momentum, which is then used to obtain a corrected mass m_{corr}. Even if the resolution of this corrected mass is poor and depends on the quality of the vertex separation (χ^2_{vtx}), it is possible to discriminate partially reconstructed backgrounds—which miss some momentum—from signal ones by applying a two-dimensional requirement in the plane defined by m_{corr} and χ^2_{vtx}, as shown in Fig. 5. This provides a significant reduction of the background contamination in electron modes, resulting in the distributions shown in Fig. 6. These still show some residual contributions from partially reconstructed backgrounds, as well as the leak of the J/ψ mode in the low mass region of the central-q^2 bin, which are included in the final invariant mass fit.

To obtain the measurement of $R_{K^{*0}}$, the likelihoods of the three hardware trigger categories are combined. The values

$$R_{K^{*0}} = \begin{cases} 0.66^{+0.11}_{-0.07}\,(\text{stat}) \pm 0.03\,(\text{syst}) \text{ for } 0.045 < q^2 < 1.1\,\text{GeV}^2/c^4 \\ 0.69^{+0.11}_{-0.07}\,(\text{stat}) \pm 0.05\,(\text{syst}) \text{ for } 1.1 < q^2 < 6.0\,\text{GeV}^2/c^4 \end{cases}, \tag{4.4}$$

are found to be compatible with the SM expectations at $2.1-2.3\sigma$ and $2.4-2.5\sigma$ for the low- and central-q^2 bins, respectively [11].

This tension, combined with the R_K measurement, points to a possible pattern of lepton flavour universality violation, which constitutes one of the most promising hints of NP to date.

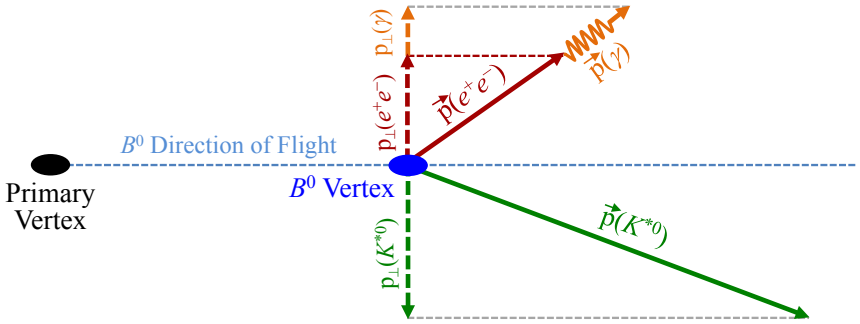

Figure 4: Sketch of the $B^0 \to K^{*0}e^+e^-$ decay. Taken from Ref. [11].

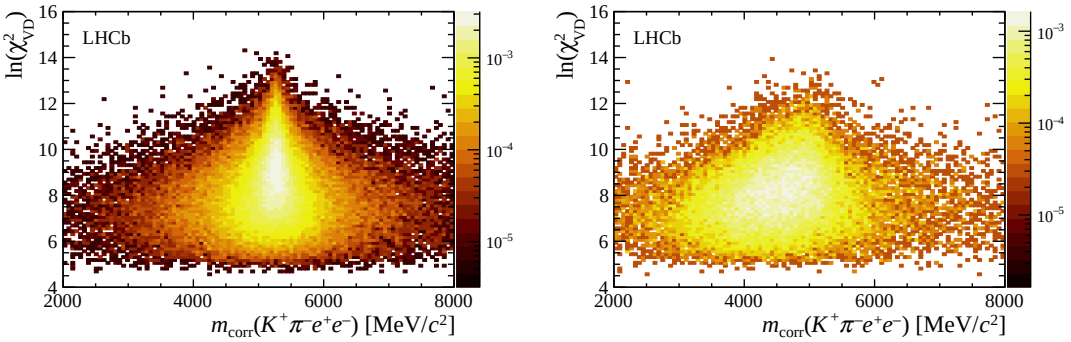

Figure 5: Two-dimensional distribution of $m_{\rm corr}$ and $\chi^2_{\rm vtx}$ for simulated (left) signal $B^0 \to K^{*0}e^+e^-$ and (right) partially reconstructed $B \to X(\to YK^{*0})e^+e^-$. Taken from Ref. [11].

To try to confirm or disprove these anomalies, updated measurements including Run II data, with larger integrated luminoisity than in Run I are being carried out. In addition, a full battery of R_X measurements is currently ongoing at LHCb, adopting a similar strategy to the one that has just been outlined for $R_{K^{*0}}$. The combination of updated R_K and $R_{K^{*0}}$ with new measurements, such as R_ϕ, $R_{K\pi\pi}$, R_{pK}, R_Λ or $R_{K^0_S}$, has the potential for NP observation at the end of the LHC Run II. Additionally, measurements of lepton flavour universality in angular distributions, specially in the case of $B^0 \to K^{*0}\ell^+\ell^-$, are underway to increase the confidence in the R_X results, thanks to their reduced sensitivity to systematic effects coming from the knowledge of the absolute scale of the electron reconstruction efficiency; work in this direction has begun with the measurement of $P_5'(\mu) - P_5'(e)$ at Belle [12].

5. Conclusions

Performing analysis involving electrons at LHCb is a challenging and nuanced task due to the low efficiency of the hardware trigger and the resolution effects due to bremsstrahlung emission. Analysis techniques have been developed to overcome these shortcomings and the various measurements obtained using data from Run I have had a large impact in the community.

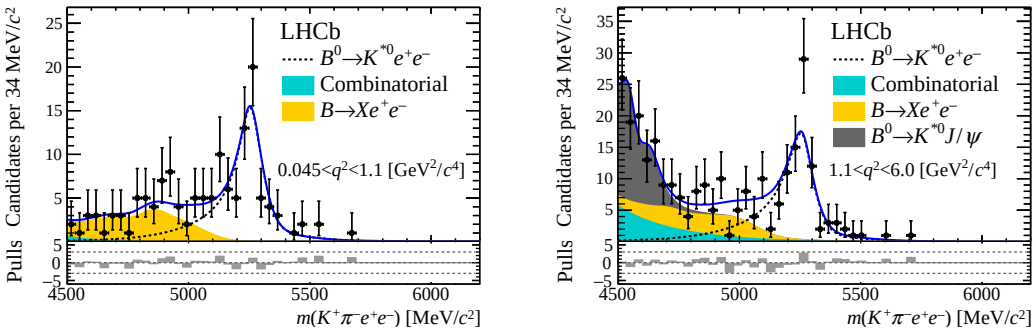

Figure 6: Fit to the invariant $K^+\pi^-e^+e^-$ mass distributions of $B^0 \to K^{*0}e^+e^-$ in the (left) low- and (right) central-q^2 bins. Taken from Ref. [11].

Besides providing some of the best constraints on the photon polarisation thanks to the angular analysis of $B^0 \to K^{*0}e^+e^-$ at very low q^2, electrons have been used to test lepton flavour universality. These measurements have resulted in tensions that add to those observed in $b \to s\mu^+\mu^-$ transitions, and currently are considered some of the most promising measurements at the LHC. With a wide array of measurements ongoing at LHCb, an observation of NP could be feasible at the end of Run II.

References

[1] S. L. Glashow, J. Iliopoulos, and L. Maiani, *Weak Interactions with Lepton-Hadron Symmetry*, Phys. Rev. **D2**, 1285–1292 (1970).

[2] LHCb collaboration, A. A. Alves Jr. *et al.*, *The LHCb detector at the LHC*, JINST **3**, S08005 (2008).

[3] LHCb collaboration, R. Aaij *et al.*, *LHCb detector performance*, Int. J. Mod. Phys. **A30**, 1530022 (2015), arXiv:1412.6352.

[4] LHCb collaboration, R. Aaij *et al.*, *Angular analysis of the $B^0 \to K^*e^+e^-$ decay in the low-q^2 region*, JHEP **04**, 064 (2015), arXiv:1501.03038.

[5] D. Becirevic and E. Schneider, *On transverse asymmetries in $B \to K^*\ell^+\ell^-$*, Nucl. Phys. **B854**, 321–339 (2012), arXiv:1106.3283.

[6] S. Jäger and J. Martin Camalich, *Reassessing the discovery potential of the $B \to K^*\ell^+\ell^-$ decays in the large-recoil region: SM challenges and BSM opportunities*, Phys. Rev. **D93**, 014028 (2016), arXiv:1412.3183.

[7] A. Paul and D. M. Straub, *Constraints on new physics from radiative B decays*, JHEP **04**, 027 (2017), arXiv:1608.02556.

[8] M. Bordone, G. Isidori, and A. Pattori, *On the Standard Model predictions for R_K and R_{K^*}*, Eur. Phys. J. **C76**, 440 (2016), arXiv:1605.07633.

[9] LHCb collaboration, R. Aaij *et al.*, *Test of lepton universality using $B^+ \to K^+\ell^+\ell^-$ decays*, Phys. Rev. Lett. **113**, 151601 (2014), arXiv:1406.6482.

[10] Heavy Flavor Averaging Group, Y. Amhis *et al.*, *Averages of b-hadron, c-hadron, and τ-lepton properties as of summer 2016*, Eur. Phys. J. **C77**, 895 (2017), arXiv:1612.07233, updated results and plots available at http://www.slac.stanford.edu/xorg/hflav/.

[11] LHCb collaboration, R. Aaij *et al.*, *Test of lepton universality with $B^0 \to K^{*0}\ell^+\ell^-$ decays*, JHEP **08**, 055 (2017), arXiv:1705.05802.

[12] Belle, S. Wehle *et al.*, *Lepton-Flavor-Dependent Angular Analysis of $B \to K^*\ell^+\ell^-$*, Phys. Rev. Lett. **118**, 111801 (2017), arXiv:1612.05014.